Renal Susceptibility Imaging in AT1 Deficient Mice

Luke Xie[1,2], Wei Li[3], Matthew Sparks[4], Yi Qi[2], Gary P. Cofer[2], Thomas Coffman[4], G. A. Johnson[1,2], and Chunlei Liu[2,3]

[1]*Biomedical Engineering, Duke University, Durham, NC, United States,* [2]*Center for In Vivo Microscopy, Duke University Medical Center, Durham, NC, United States,* [3]*Radiology, Duke University Medical Center, Durham, NC, United States,* [4]*Nephrology, Duke University Medical Center, Durham, NC, United States*

Introduction

Quantitative susceptibility imaging has been shown to be an invaluable tool in neuroimaging using MRI. Susceptibility imaging has higher CNR compared to magnitude, especially at higher fields, and is particularly sensitive to the spatial variation of chemical composition and microstructure (1). Similar to the brain, the kidney is a highly structured organ; the kidney has numerous tubules and vessels that depends on the stability of macromolecules and contains many paramagnetic materials that have high susceptibility. In kidneys with altered morphology, the changed spatial distribution of these paramagnetic materials can lead to significant changes in the magnetic susceptibility. In this study, we explored the application of susceptibility imaging to assess altered kidneys from genetically modified mice that lack angiotensin II receptor AT1A (Agtra -/-) or both AT1A and AT1B receptors (Agtr1a -/- Agtr1b -/-). AT1 receptors respond to the vasoconstricting stimulus of angiotensin II, which is a major target for lowering blood pressure. The mice in this study had no systemic pressor response to angiotensin II. Furthermore, the kidneys in these mice exhibit thickening of arterial walls, focal areas of interstitial fibrosis, and tubular atrophy (3). To quantify susceptibility changes in altered kidneys, we characterized these values in the cortex, outer medulla, and inner medulla for comparison in the wild type, Agtr1a -/-, and combined Agtr1a -/- Agtr1b -/- mice. Significant differences in the mean and the distribution of susceptibilities were observed among the three types of mice.

Methods

Animal preparation: Mice used in this study were C58Bl/6 wild type (WT, n=5), single isoform homozygous Agtr1a -/- (A, n=5), and double homozygous Agtr1a -/- Agtr1b -/- (AB, n=5). Biological support: Mice were anesthetized under isolfurane. Conventional transcardiac fixation was used for perfusion. The animals were perfused with saline and 0.1% heparin at 8 ml/min for 5 mins, and then perfused with 50 mM ProHance dissolved in 10% formalin at 8 ml/min for 5 mins. Kidneys were stored in 2.5 mM ProHance and 10% formalin for 24 hours before imaging. MRI and Analysis: Kidneys were fit in an acrylic holder filled with fomblin and scanned on a 9.4 T system (400 MHz Oxford superconducting magnet) using a gradient echo sequence (TR=50ms, TE=4.4ms, FA=60°, and resolution=31μm). The local phase in the kidney images was extracted using a Laplacian-based 3D phase unwrapping; the background phase was removed with a sphere-mean-value filter; susceptibility was then calculated using the LSQR method (2). The susceptibility values were then compared between the 3 groups (n=5 each for WT, A, AB) for each of the kidney regions (cortex, outer medulla, and inner medulla).

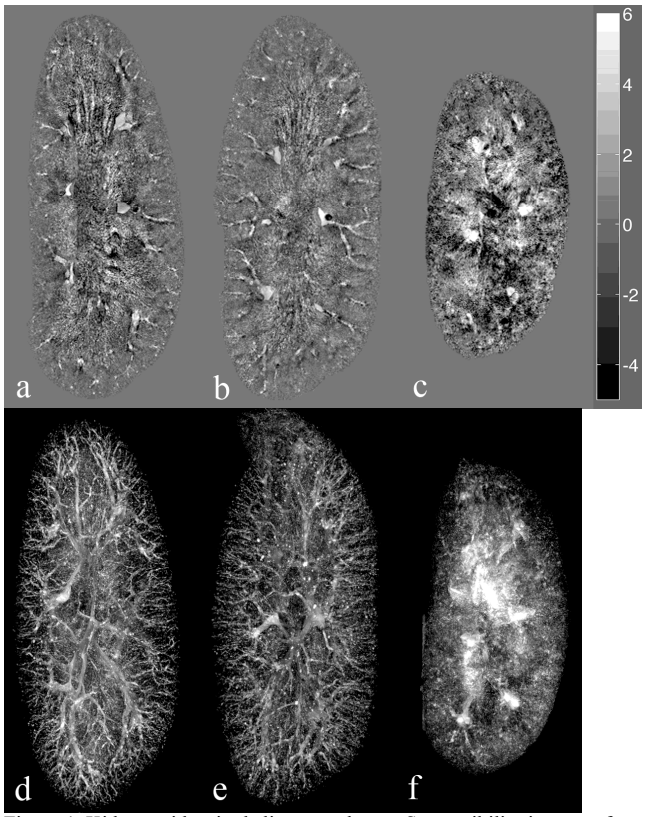

Figure 1. Kidney midsagittal slices are shown. Susceptibility images of a wild type, AT1a -/-, and AT1a -/- AT1b -/- mouse are shown in a), b), and c), respectively. These are windowed from -5 to 6 ppm. MIPs of susceptibility of the same kidneys are shown in d), e), and f), respectively.

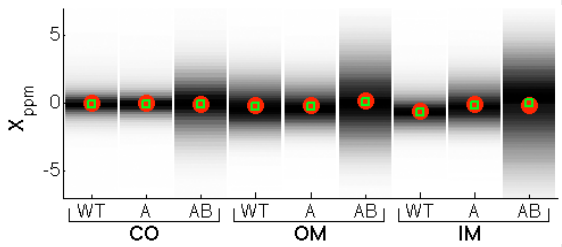

Figure 2. Distribution plots of susceptibility in the cortex (CO), outer medulla (OM), and inner medulla (IM). These distributions are taken from the regions of a single wild type (WT), AT1a -/- (A), and AT1a -/- AT1b -/- (AB) mouse. Red circle are means and green squares are medians.

	WT	A	AB
CO	-0.12 ± 0.12	-0.14 ± 0.19	**0.52 ± 0.22**
OM	-0.16 ± 0.20	-0.46 ± 0.25	**-0.30 ± 1.27**
IM	-0.17 ± 0.40	-0.12 ± 0.79	**0.38 ± 0.74**

Table 1. Susceptibility values from 3 kidney regions: CO, OM, and IM. The mean and standard deviation are taken from the regions of the wild type (WT, n=5), AT1a -/- (A, n=5), and AT1a -/- AT1b -/- (AB, n=5).

Results

Susceptibility images of the WT, A, and AB kidneys are shown in Figure 1 a, b, and c, respectively. MIPs of the images of the same kidneys are shown in Figure 1 d, e, and f, respectively. The WT and A kidneys have normal oblong shapes, distinct renal regions, and highly contrasted vessels. However, AB kidneys have shorter long axes, shrunken shapes, and coarse surfaces. The renal regions and vessels are not well defined. Susceptibility values of AB kidneys have a much broader range compared to the WT and A kidneys, as shown in the distribution plots in Figure 2. Sample distribution plots were taken from all 3 regions of a single WT, A, and AB kidney. The susceptibility values of all 15 datasets are included in Table 1. The mean and standard deviation were determined from an averaged ROI in the cortex (CO), outer medulla (OM), and inner medulla (IM) for all 5 kidneys in each of the 3 mouse groups. Overall, the AB group has higher susceptibility values, which indicates more paramagnetic material.

Discussion and Conclusion

Susceptibility quantification allowed us to obtain higher quality and higher contrast images in the WT and A kidneys. Values were quantified and compared between all regions (cortex, outer medulla, and inner medulla) for all groups (WT, A, and AB). The susceptibility values in the AB kidneys were generally higher and more broadly distributed, resulting in reduced susceptibility contrast in kidney structures. Macromolecules and paramagnetic material in the vessels, tubules, and collecting ducts may no longer be intact compared to a normal kidney. Diverse and diffuse fibrosis and tubular atrophy (3) may also lead to decreased susceptibility contrast. On the other hand, focal regions of cortical defect and interstitial inflammation may explain the increase of more, but dispersed, paramagnetic material or higher susceptibility values. These regions of fibrosis and inflammation must be validated using specific histological stains and compared with susceptibility images. Nonetheless, susceptibility imaging for highly ordered structures such as the kidney has produced excellent quantitative images and is promising in the field of renal MRI imaging.

Acknowledgements

All work was performed at the Duke Center for In Vivo Microscopy and is funded by NCRR P41RR005959, NCI U24CA092656, and NIBIB T32GM008555.

References

[1] Li W., Wu B., Liu, C. (2011). *NeuroImage*, **55**, 1645-1656. [2] Liu, C. (2010). *Magn Reson Med*, **63**(6), 1471-1477. [3] Oliverio et al. (1998). *Proc Natl Acad Sci*, **95**(26): 15496-501.